

PAPER • OPEN ACCESS

Rapid solidification of Al-Cu droplets of near eutectic composition

To cite this article: A-A. Bogno *et al* 2019 *IOP Conf. Ser.: Mater. Sci. Eng.* **529** 012021

View the [article online](#) for updates and enhancements.

Rapid solidification of Al-Cu droplets of near eutectic composition

A-A. Bogno¹, J. Valloton¹, D.D. Jimenez¹, M. Rappaz², H. Henein¹

¹ Department of Chemical and Materials Engineering
University of Alberta, Edmonton, AB T6G 2G6 Canada

² Institute of Materials, Ecole Polytechnique Fédérale de Lausanne
CH-1015 Lausanne Switzerland

Email: bogno@ualberta.ca / hhenein@ualberta.ca

Abstract. Near eutectic Al-Cu droplets were rapidly solidified by Impulse Atomization. A wide range of microstructural scales was obtained at different cooling rates and undercoolings. The micrographs of the investigated samples revealed two distinct zones of different structural morphologies: An undulated eutectic morphology developed during recalescence following the single grain nucleation and a regular lamellar eutectic morphology resulting from the solidification of the remaining liquid post recalescence. The volume fraction of each zone was measured as a function of the droplet diameter, and the nucleation undercooling was deduced using the hypercooling limit equation. Scanning Electronic Microscopy imaging and microhardness measurements were used to evaluate the microstructural scale, and mechanical properties.

1. Introduction

High undercooling / cooling rate associated with rapid solidification of metallic alloys results in various beneficial microstructural features. These include minimal segregation, grain refinement, solubility extension and the formation of metastable phases [[1]][[2]][[3]][[4]]. Thus, in recent decades, rapid solidification techniques have been extensively used to develop new advanced materials. However, it is sometimes difficult to relate the observed microstructure with process parameters due to experimental difficulties. These include, measurements of variables such as cooling rate, undercooling and solidification rate, which are very well known to control the final solidification microstructure.

Rapid solidification of alloys of eutectic composition is important from both technological and scientific points of view as it can result in very fine microstructures and metastable phases. The Al-Cu eutectic system has been extensively studied and various types of microstructures have been reported to form under rapid solidification conditions, depending on the solidification rate [[5]][[6]][[7]][[8]]. At low cooling rates, a regular lamellar eutectic structure, consisting of alternate α -Al and θ -Al₂Cu lamellae, is formed. After nucleation the two phases grow cooperatively with a fairly well-established relationship between the solidification rate V and the interlamellar spacing λ , given by the equation $V\lambda^2 = \text{constant}$ [[9]]. At higher cooling rates, Al-Cu eutectic solidifies into degenerate / anomalous eutectic structure consisting of irregular θ -Al₂Cu precipitates embedded in an α -Al matrix or into undulated eutectic



microstructures, where α -Al and θ -Al₂Cu lamellae become wavy [[5]][[6]]. At even higher cooling rates, a banded eutectic [[5]][[10]] or a fully supersaturated single α -Al solid solution were observed [[11]][[12]].

This paper presents the observations made on rapidly solidified Al-Cu droplets of eutectic composition, obtained by Impulse Atomization (IA). This single fluid atomization technique yields solidification microstructures formed over a wide range of undercooling, from the onset to the end of recalescence and during further cooling.

2. Materials and methods

Near-eutectic Al-Cu droplets were generated using IA. Aluminum and copper were melted in a graphite crucible by heating up to 1200 °C. Atomization was achieved under a stagnant argon atmosphere with oxygen level less than 20ppm. The melt was superheated to 750°C, i.e., about 200°C above the equilibrium eutectic temperature. A wide range of droplet sizes (< 200 μ m to 1000 μ m) were obtained to ensure microstructural analysis over a wide range of cooling rates and undercoolings.

The composition of the eutectic droplets (given in the table below) were obtained by chemical analysis performed according to ASTM E1097-12 and ASTM E1479-16. As can be noted, both alloys are slightly hypoeutectic, hence the near-eutectic designation.

Sample ID	Al	Cu	Si	Fe	Zn
Alloy 1	Balance	31.9	0.01	<0.01	None
Alloy 2	Balance	32.2	None	0.02	0.04

The as-atomized microstructures were characterized by Scanning Electron Microscopy (SEM) using both Secondary Electrons (SE) and Back Scattered Electrons (BSE) modes, on both ground and polished sections of the droplets as well as on their as-atomized external surface. The instrument used was a Zeiss Sigma Field Emission SEM equipped with a Bruker energy dispersive X-ray spectroscopy (EDS) system with dual silicon drift detectors, each with an area of 60 mm² and a resolution of 123 eV.

The scale of the microstructure was determined by eutectic spacing measurement using line intercept method on the micrographs, according to ASTM E112-13. The strength of the samples was evaluated through microhardness measurement using a Buehler VH 3100 microhardness machine. The device was calibrated using a manufacturer provided steel block. Five indentations were randomly applied on each sample with a load of 100gf held for 10s.

3. Results

3.1. Nucleation and microstructure formation

Figures 1a through 1f show typical micrographs of as-atomized droplets surface and cross-sections of the two investigated alloys. The BSE imaging providing an atomic number (Z) contrast, α -Al appears dark while the Cu rich θ -Al₂Cu phase is in light grey. As shown in Figure 1, the majority of the investigated droplets have a single nucleation point from where the microstructure propagates. Furthermore, the nucleation point is most often located at the surface of the atomized droplets, but in some cases it can be within the volume, as is for example the case for the Alloy 2 shown in (e). Nucleation usually occurs in two steps, i.e., the nucleation of one phase helps that of the second one, as shown in (e) and (f). Once both phases are formed, the coupled eutectic grows with a very undulated morphology corresponding to Zone A in the figure, followed by a regular eutectic in Zone B.

Zone A, formed around the nucleation point, which in most cases is an impurity, is characterized by an undulated eutectic morphology. The solidification speed of the eutectic front in this region is assumed to be very high, since it forms during the recalescence period. In some of the droplets, as shown in Figure 1e, primary nucleation occurs with a Cu-rich region (Figure 1f), which then grows as a dendrite before coupled eutectic growth occurs. The elemental composition of this dendrite, confirmed by EDX,

corresponds to that of the θ -Al₂Cu phase. As the melt surrounding this growing dendrite is depleted of Cu, there is a driving force to form α -Al. This is clearly shown in the zoom of Figure 1f (dark layer surrounding the θ -dendrite). Once both phases are formed, the undulated eutectic forms.

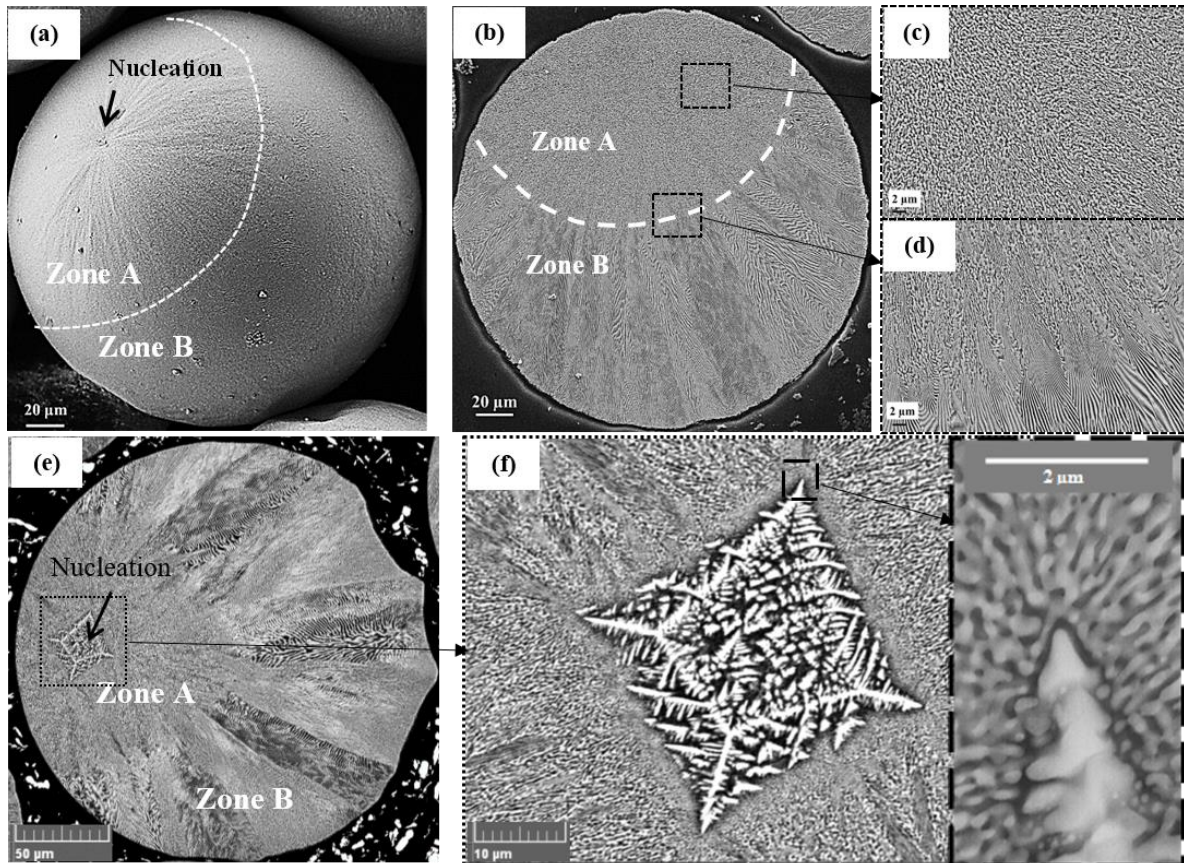


Figure 1: SEM (BSE) micrographs of the two investigated eutectic alloys. (a) Surface of a 215 μm diameter droplet from Alloy 1, the nucleation point is indicated on the surface by an arrow. (b) The corresponding cross section of the droplet showing the undulated microstructure (Zone A) and the regular lamellar structure (Zone B). Magnifications of Zone A and of the transition between Zones A and B are shown in (c) and (d), respectively. (e) Cross section of a 230 μm droplet from Alloy 2. The microstructure propagated from the Cu-rich dendrite (nucleation point) to a Zone A (undulated eutectic) which then becomes a regular lamellar structure (Zone B). (f) Magnification of the transition between the Cu-rich dendrite (light grey) and the undulated eutectic, with formation of an α -Al layer in between.

These observations are similar to those of laser remelting of the irregular eutectic Al-Si, i.e., formation of Si first, with an α -Al layer around it that grows before coupled growth occurs [[13]]. However, in this last case, this sequence of phase formation could be expected since this is an irregular eutectic and the composition was hypereutectic. It is well known that irregular eutectics have a coupled zone skewed toward the faceted phase, i.e., silicon [[14]]. But Al-Cu is a regular eutectic, i.e., both α -Al and θ -Al₂Cu are non-faceted (this is quite evident for the θ -phase in Figure 1(f)). Since the coupled zone should not be skewed toward either phase, it is hard to predict which phase has a growth advantage at large undercooling. Considering Jackson's criterion for the formation of a faceted phase, the entropy of fusion ΔS_f for the θ -phase has been calculated with Thermo-Calc [[15]] and the thermodynamic database TTA17. It is equal to 17.5 J mol⁻¹K⁻¹ at 869 K, thus giving $\Delta S_f \approx 2R$, where R is the gas constant. This means that the stable θ -phase is close to being a faceted phase according to this criterion and the coupled

zone might be skewed toward θ . For a eutectic composition, this would rather predict the formation of α and not θ . It should be recalled that the concept of coupled zone is solely based on a growth competition undercooling advantage, and not at all on nucleation. Further analyses are required to see if primary nucleation of Al_2Cu is induced by trace elements (in this case Fe and Zn).

Once both phases are present, they grow in a coupled but very unstable way in Zone A, thus producing an undulated microstructure at large undercooling. Once the recalescence ends and the undercooling is reduced, there is a transition to the expected regular lamellar eutectic structure of Al- Al_2Cu (Zone B). It is worth noting that Zone B consists of eutectic colonies, characteristic of eutectic structures resulting from the rejection of impurities (Si, Fe or Zn in this case) during solidification [[16]]. The colonies could also have their origin from a thermal instability as the growth, at least during recalescence, occurs in an undercooled melt (i.e., negative thermal gradient).

3.2. Nucleation undercooling

Zone A is assumed to have formed under conditions dominated by internal heat flow under adiabatic conditions during recalescence. Numerical simulations indeed show that recalescence is very fast (less than 5% of the total solidification time account for primary phase nucleation and growth during recalescence [[14]]) and that heat losses of the droplet can be neglected. Under such conditions, the nucleation undercooling, ΔT_N , can be defined by Eq. 1, i.e., by the product of the solid fraction f_R formed during recalescence and the characteristic hypercooling limit of the melt, ΔT_{hyp} .

$$\Delta T_N = f_R \cdot \Delta T_{hyp} \quad (\text{Eq.1})$$

$$\Delta T_{hyp} = \frac{\Delta H_f}{C_p^l} \quad (\text{Eq.2})$$

where C_p^l ($2.86 \times 10^6 \text{ Jm}^{-3}\text{K}^{-1}$) and ΔH_f ($1.23 \times 10^9 \text{ Jm}^{-3}$) are the melt heat capacity and the latent heat of fusion, respectively (values are taken from [[17]]).

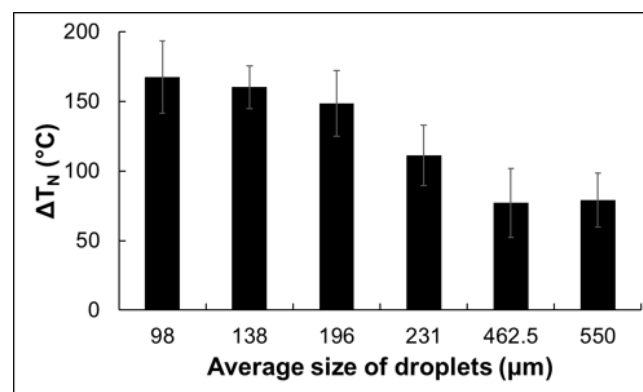


Figure 2: Variation of nucleation undercooling with average droplet size for Al-Cu of eutectic composition, sample ID: Alloy 1

Figure 2 shows the variation of nucleation undercooling with respect to the average droplet size. The results are obtained based on the measurement of the volume fraction of Zone A of the samples for Alloy 1 where nucleation occurred on the droplet surface. Figure 2 shows that the nucleation undercooling in each droplet is fairly large, which explains the formation of the undulated microstructure in Zone A, promoted by high growth rate (0.2 to 0.5 ms^{-1}) as observed in rapid solidification microstructure of Al-Cu eutectic alloy obtained by laser remelting [[5]].

3.3. Scale of the microstructures and mechanical properties

The eutectic spacing, λ , was measured for each droplet as a function of the normalized position (Z/D) on each investigated droplet of diameter D , where Z is the distance from the nucleation point along the growth direction within the two zones. In Zone B, the measurement of the average lamellar spacing was carried out on the finer eutectic colonies only, in order to minimize stereological effects of the lamellae orientation in 2-dimensional cross sections. In Zone A, the interphase spacing λ was measured from a mean intercept. Figure 3a shows the variation of the average eutectic spacing with the normalized position (Z/D) on each investigated droplet of alloy 1. Similar results were obtained for Alloy 2.

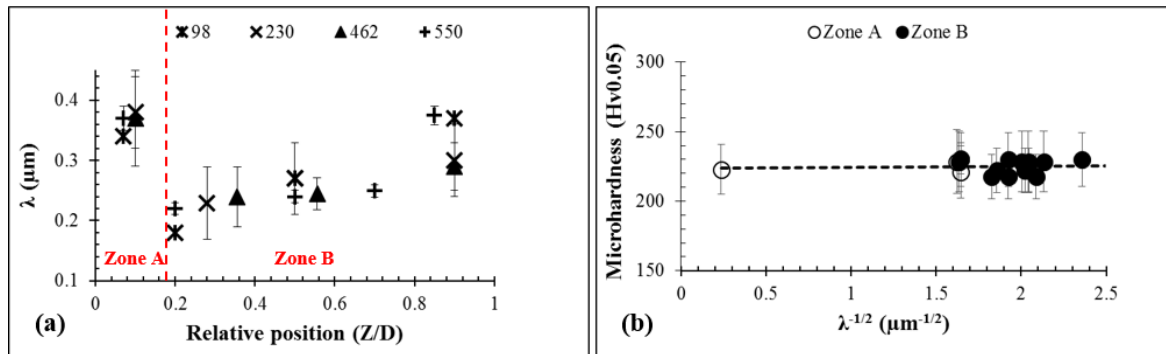


Figure 3. (a) Spatial variation of interphase (Zone A) and lamellar (Zone B) spacing λ as a function of the normalized distance Z/D from the nucleation point. (b) Hall-Petch relationship between microhardness and $\lambda^{-1/2}$.

In Zone B, the average lamellar spacing increases with Z as expected. After recalescence, the eutectic front interface velocity V is controlled by the heat flow extracted from the droplet during the nearly isothermal eutectic reaction. As the solid-liquid interface increases, V has to decrease to keep the latent heat release about constant, thus explaining the increase in λ with the relationship $\lambda^2 V = \text{constant}$. Surprisingly, the interphase spacing λ in Zone A is nearly constant (within the error bars), regardless of the droplet size, and larger than the lamellae spacing measured in Zone B. This should be the opposite since the undercooling during recalescence is substantially larger than during the nearly isothermal plateau. This observation, also reported during laser remelting (but not explained) in [[5]], is not well understood but clearly shows that the growth kinetics of these two microstructures is different.

Finally, Figure 3b shows the average microhardness measured as a function of $\lambda^{-1/2}$, describing the Hall-Petch relationship associated with one of the two eutectic phases [[18]]. Assuming that it is the α -Al that deforms plastically, dislocations could be stopped by the interfaces with the θ - Al_2Cu phase, hence microhardness could depend on the eutectic spacing. However, microhardness is found to be constant around 220 ± 10 HV within both Zones A and B, independently of the investigated droplet size. It is worth noting that there is $\sim 50\%$ in volume of α -Al and θ - Al_2Cu in both Zone A and Zone B, based on measurement performed on the 2-dimensional cross sections of all the investigated samples.

4. Summary

Impulse Atomization was used to investigate microstructure development in rapidly solidified Al-Cu droplets of near-eutectic composition as a function of cooling rate (droplet size). From microscopy analysis, evidence of a single nucleation point on the surface was found for all the investigated samples. Two types of eutectic morphologies have been observed: an undulated eutectic during recalescence and a regular lamellae structure during nearly isothermal solidification after recalescence. From the volume of the undulated eutectic zone, assumed to occur during adiabatic recalescence, the nucleation undercooling could be determined and was found to vary between 80 K and 170 K, depending on the droplet size. While the eutectic spacing of Zone B seems to follow the $\lambda^2 V$ relationship typical of

eutectic, the interphase spacing of Zone A is surprising. It is almost independent of the droplet size (and thus undercooling) and larger than the lamellae spacing of Zone B. Further investigations need to be done to understand the growth kinetics of this morphology, which is definitely not like $1-\lambda$ or $2-\lambda$ oscillations reported in the literature [[5]][[19]]. Also, 3-dimensional characterization of Zone A is an ongoing effort.

Acknowledgements

The authors are grateful to the Natural Sciences and Engineering Research Council of Canada (NSERC) and the European Space Agency (ESA) for their financial support. Dr. Mark Gallerneault of Alcerco Inc. is also acknowledged for providing the aluminum raw materials. Finally, thanks are due to Dr. Jose Eduardo Spinelli for fruitful discussions.

References

- [1] Kear, B.H., and Giessen, B.C., 1982, *MRS Bull.*, **7**, (02), 5.
- [2] Bogno, A.-A., Riveros, C., Henein, H., and Li, D., 2016, *Metall. Mater. Trans. B - Process Metall. Mater. Process. Sci.*, **47**, (6), 3257.
- [3] Banerjee, S., and Dey, G.K., 2004, *J. Mater. Sci.*, **39**, (12), 3985.
- [4] Liu, R.P., Herlach, D.M., Vandyoussefi, M., and Greer, A.L., 2004, *Metall. Mater. Trans. A*, **35**, (2), 607.
- [5] Zimmermann, M., Carrard, M., and Kurz, W., 1989, *Acta Metall.*, **37**, (12), 3305.
- [6] Mueller, B.A., and Perepezko, J.H., 1988, *Mater. Sci. Eng.*, **98**, 153.
- [7] Lee, S.M., and Hong, C.P., 1998, *ISIJ Int.*, **38**, (2), 157.
- [8] Sahoo, S., and Ghosh, S., 2015, *Appl. Phys. A Mater. Sci. Process.*, **121**, (1), 45.
- [9] Jackson, K.A., and Hunt, J.D., 1966, *Trans. Am. Inst. Min. Engrs.*, **236**, 1129.
- [10] Zimmermann, M., Carrard, M., Gremaud, M., and Kurz, W., 1991, *Mater. Sci. Eng. A*, **134**, 1278.
- [11] Williams, D.B., and Edington, J.W., 1976, *Philos. Mag. A J. Theor. Exp. Appl. Phys.*, **34**, (2), 235.
- [12] Scott, M.G., and Leake, J.A., 1975, *Acta Metall.*, **23**, (4), 503.
- [13] Gremaud, M., Allen, D.R., Rappaz, M., and Perepezko, J.H., 1996, *Acta Mater.*, **44**, (7), 2669.
- [14] Bogno, A.-A., Khatibi, P.D., Henein, H., and Gandin, Ch-A., 2016, *Metall. Mater. Trans. A Phys. Metall. Mater. Sci.*, **47A**, (9), 4606
- [15] Andersson, J.O., Helander, T., Höglund, L., Shi, P., and Sundman, B., 2002, *Calphad Comput. Coupling Phase Diagrams Thermochem.*, **26**, (2), 273.
- [16] Rutter, J.W., 1977, *J. Cryst. Growth*, **42**, 515.
- [17] Zimmermann, M., 1990, "Solidification rapide de l'eutectique Al-Al₂Cu par refusion laser," *Institute of Materials, Ecole Polytechnique Fédérale de Lausanne*.
- [18] Mason, D.P., and Van Aken, D.C., 1993, *Scr. Metall. Mater.*, **28**, (2), 185.
- [19] Karma, A., 1987, *Phys. Rev. Lett.*, **59**, (1), 71.